How representative is Svalbard for future Arctic climate evolution? An Earth system modelling perspective (SvalCLIM)

Ada Gjermundsen[1], Lise Seland Graff[1], Mats Bentsen[2], Lars Anders Breivik[1], Jens Boldingh Debernard[1], Risto Makkonen[3,4], Dirk J.L. Olivié[1], Øyvind Seland[1], Paul Zieger[5], and Michael Schulz[1,6]

1 Norwegian Meteorological Institute, Henrik Mohns plass 1, 0313 Oslo, Norway
2 NORCE Norwegian Research Centre and Bjerknes Centre for Climate Research, Nygårdsgaten 112, 5008 Bergen, Norway
3 Climate System Research, Finnish Meteorological Institute, P.O. BOX 503 FI-00101 Helsinki, Finland
4 INAR – Institute for Atmospheric and Earth System Research P.O. Box 64 00014 University of Helsinki, Finland
5 Department of Environmental Science, Stockholm University 106 91 Stockholm, Sweden
6 University of Oslo, Department of Geosciences, P.O. Box 1047 Blindern, 0316 Oslo, Norway

Corresponding author: Ada Gjermundsen, adag@met.no
ORCID number 0000-0002-2053-4689

K**eywords:** Earth system modelling, Arctic amplification, historical trends, future projections

DOI: https://doi.org/10.5281/zenodo.4034104

1. Introduction

It is well known that the world has become warmer in response to emissions of anthropogenic greenhouse gases (GHGs). This warming is however not evenly distributed across the globe, but is amplified in specific regions, such as in the Arctic. This, can for instance, be seen in temperature records from the Svalbard Archipelago, which reveal the greatest increase in temperature in Europe over the last three decades (Nordli et al. 2020).

The amplification of the Arctic temperature signal compared to the global mean is known as Arctic amplification (AA). It is most pronounced during winter and has large ramifications for the cryosphere, the hydrological and biogeochemical cycles and for all life in the Arctic (Meier et al. 2014; Bintanja and Selten 2014; Kim et al. 2019). AA is not merely a result of climate variability (Winton 2011; Notz and Marotzke 2012; Liang et al. 2020), but can be attributed to a number of mechanisms, including changes in surface albedo (associated with melting snow and sea ice), clouds, the vertical distribution of temperature, and hence in the lapse rate, water-vapour content, surface fluxes, and atmospheric and oceanic energy transports (Screen and Simmonds 2010; Doyle et al. 2011; Serreze and Barry 2011; Pithan and Mauritsen 2014; Simpkins 2017; Screen and Blackport 2019). It has also been shown that the surface temperature in the Arctic and in Svalbard can be affected by remote anthropogenic emissions such as of European sulfur (Navarro et al. 2016) and North-Eurasian black carbon (Sand et al. 2013). However, a quantitative understanding of the individual mechanisms contributing to AA is not well known. Specifically in Svalbard, the warming is in part linked to changes in the atmospheric circulation due to extensive sea-ice melt in the fjords and the surrounding ocean (Isaksen et al. 2016; Dahlke et al. 2020).

Being situated in the Arctic and in a region with relatively pristine conditions, Svalbard is a very important and interdisciplinary observational supersite for the Arctic. However, little attention has been paid to how representative observations from Svalbard are for the entire Arctic region, and studies that compare observations from different sites located in the Arctic suggest that persistent differences beyond year-to-year variability can occur (Freud et al. 2017; Ding et al. 2018; Schmeisser et al. 2018). Here, we investigate how representative Svalbard is for the Arctic region as a whole, using data from numerical simulations with climate models. We assess recent and future changes and trends in the climate in Svalbard, comparing them to corresponding results from the entire Arctic region and to global results.

Climate models are excellent tools for understanding, in a consistent manner, both the global and regional climate. They are mathematical representations of the climate system based on physical, biological, and chemical principles. The models solve the governing equations of the climate system numerically in order to, for instance, simulate future climate scenarios on a 3D-grid (height, latitude, longitude) and consist of several components (e.g. atmosphere, ocean, land, sea ice, vegetation), which interact by transfer of energy, momentum, humidity, and matter. When such a model also includes interactive atmospheric chemistry and biogeochemistry (e.g. the carbon cycle), it is called an *Earth System Model* (ESM).

The spatial and temporal scales of the model components determine which processes are resolved. Processes occurring on even smaller scales than that resolved by the models (so-called sub-grid processes), biological processes, and chemical interactions need to be represented either by mathematical models that capture the essence of the behaviour of the phenomenon or by empirical functions deduced from instance measurements. Examples of such processes are boundary-layer convection, aerosol-cloud interactions, turbulence, oceanic internal- and gravity waves, and molecular processes. Because parameterisations typically only capture first-order effects and are often not valid under all possible conditions, they represent a large source of uncertainties in the models.

ESMs are not constrained by observations in the same way as, for instance, weather prediction models and reanalysis data. ESMs start from an initial state, which can be based on observations or data from a previous ESM run; then they run freely while being forced by solar insolation, GHG concentrations, natural aerosols and chemical species (highly model dependent), emissions from volcanoes, anthropogenic aerosol and GHG emissions, and changes in land use. Such forcing information is given at the temporal and spatial resolution that best represents current knowledge.

In this study, we use data from a large set of state-of-the-art ESMs participating in phase 6 of the Coupled Model Intercomparison Project (CMIP6; see info box for a more detailed description). We consider data from a vast number of different experiments, including a simulation of the historical period 1850–2014 (Section 2) and projections of future climate change (Section 3). To investigate how realistic the historical simulations are, we compare the model data to several reanalysis products, observationally based global data sets, and to local observations from Svalbard. Reanalysis combine advanced forecast modelling and observations (through data assimilation) to produce a coherent estimate of the recent history of the Earth system and that differs fundamentally from earth system modelling as the former are constrained by the observations, while the latter run freely. See the Data availability section for further details.

INFO BOX: COUPLED MODEL INTERCOMPARISON PROJECT PHASE 6 (CMIP6)

CMIP is a project of the World Climate Research Programme (WCRP)'s Working Group of Coupled Modelling (WGCM), which coordinates climate model experiments, including future scenarios that are considered in the assessment reports by the Intergovermental Panel of Climate Change (IPCC), involving 33 international modelling teams and more than 70 ESMs; defines common protocols for experiments, forcings, and output to advance scientific understanding of the Earth System; develops experiment sets in phases and is currently in the 6th phase.

The experimental design focuses on three broad scientific questions (Eyring et al. 2016): (1) How does the Earth System respond to forcing? (2) What are the origins and consequences of systematic model biases? (3) How can we assess future climate changes given climate variability, predictability and uncertainties in scenarios?

The CMIP6 experiments consist of a set used to assess the equilibrium state of the ESMs and their sensitivity to idealized changes in CO_2 (the so-called DECK experiments) and historical experiments in which the models are run with observed forcings to recreate the recent historical period (for CMIP6, it is 1850–2014) and 23 different more specialized sets known as model intercomparison projects "MIPs", which are tailored to investigate more specific questions such as, for instance, how the Earth system responds to polar amplification (Polar Amplification MIP; Smith et al. 2019).

Experiments used in this report: Simulations of the pre-industrial (taken as year 1850) climate, the historical experiment described above, and simulations of future scenarios (from ScenarioMIP) for the years 2015–2100.

For more information, see Eyring et al. 2016, the CMIP6 webpages [1,2], and Eyring et al. 2018.

1 https://www.wcrp-climate.org/wgcm-cmip/wgcm-cmip6
2 https://pcmdi.llnl.gov/CMIP6/

2. Historical trends in temperature, precipitation and sea ice

We consider 3 regions: Svalbard, the entire Arctic, and the globe. *Svalbard* is here defined as the region bounded by 70°N – 83°N, 20°W – 50°E (inner dashed red box in Figure 1). This does include rather large parts of the surrounding ocean, but we find comparable results when using a smaller region that is more confined to the Svalbard Archipelago (indicated by the blue dashed box in Figure 1), albeit with substantially larger variability. Thus, the results presented in this section are from the extended Svalbard region (red box). The *Arctic* is defined as the area within 66°N – 90°N (outer red dashed circle).

We consider recent changes and trends in near-surface (2 m) temperature, precipitation, and sea-ice extent for our three focus regions, using data from the CMIP6 historical experiment from 48 different ESMs (Figure 1) that all performed this experiment. The historical experiment covers 1850–2014, but we focus on the last decades to facilitate more direct comparison with reanalysis products and observations.

2.1. Near-surface temperature

The AA of the near-surface temperature is evident in both observations and models (Figure 2) for all seasons except summer (defined as June, July, and August; JJA), with the warming being most intense during autumn (September, October, and November; SON) and winter (December, January, and February; DJF). The enhanced winter warming compared to summer is largely caused by transport of water vapour by the atmosphere (Doyle et al. 2011; Simpkins 2017; Lee et al. 2017) and by enhanced ocean heat release in response to thinner sea ice and reduced sea-ice extent (Screen and Simmonds 2010; Kim et al. 2019; Cohen et al. 2020).

Figure 2 shows the historical (years 1985–2014) seasonally averaged anomalies against the baseline (years 1951–1980) for near-surface (2 m) temperature, as found in the observationally based temperature data-set GISTEMPv4 (upper) and the CMIP6 ensemble mean (middle). Generally, the

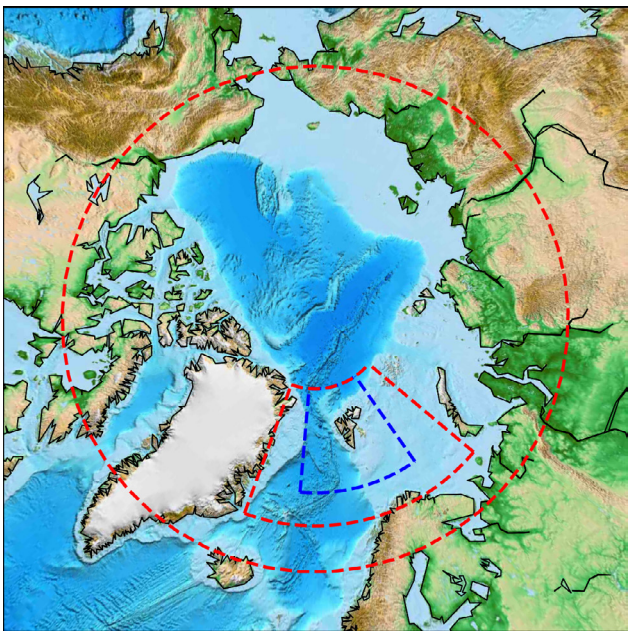

1 ACCESS-CM2	17 CNRM-CM6-1	33 INM-CM5-0
2 ACCESS-ESM1-5	18 CNRM-CM6-1-HR	34 IPSL-CM6A-LR
3 AWI-CM-1-1-MR	19 CNRM-ESM2-1	35 KACE-1-0-G
4 AWI-ESM-1-1-LR	20 E3SM-1-0	36 MIROC6
5 BCC-CSM2-MR	21 E3SM-1-1	37 MIROC-ES2L
6 BCC-ESM1	22 EC-Earth3	38 MPI-ESM-1-2-HAM
7 CAMS-CSM1-0	23 EC-Earth3-Veg	39 MPI-ESM1-2-HR
8 CanESM5-CanOE	24 EC-Earth3-Veg-LR	40 MPI-ESM1-2-LR
9 CanESM5	25 FGOALS-f3-L	41 MRI-ESM2-0
10 CAS-ESM2-0	26 GFDL-ESM4	42 NESM3
11 CESM2-FV2	27 GISS-E2-1-G-CC	43 NorCPM1
12 CESM2	28 GISS-E2-1-G	44 NorESM2-LM
13 CESM2-WACCM-FV2	29 GISS-E2-1-H	45 NorESM2-MM
14 CESM2-WACCM	30 HadGEM3-GC31-LL	46 SAM0-UNICON
15 CIESM	31 HadGEM3-GC31-MM	47 TaiESM1
16 CMCC-CM2-SR5	32 INM-CM4-8	48 UKESM1-0-LL

Figure 1: Indicated by the red dashed lines are the regions used for the comparison in this report (left). The Arctic is defined as 66°N–90 °N (outer red circle). Svalbard is defined as 70°N-83°N, 20°W-50°E (inner red circle). A narrower region around Svalbard, confined to 73°N-83°N, 5°W-35°E, was included in a sensitivity test (blue dashed line). The names of the 48 ESMs that are part of the CMIP6 ensemble and analysed in this chapter; the number and coloured dots are used in the following scatter plots (right).

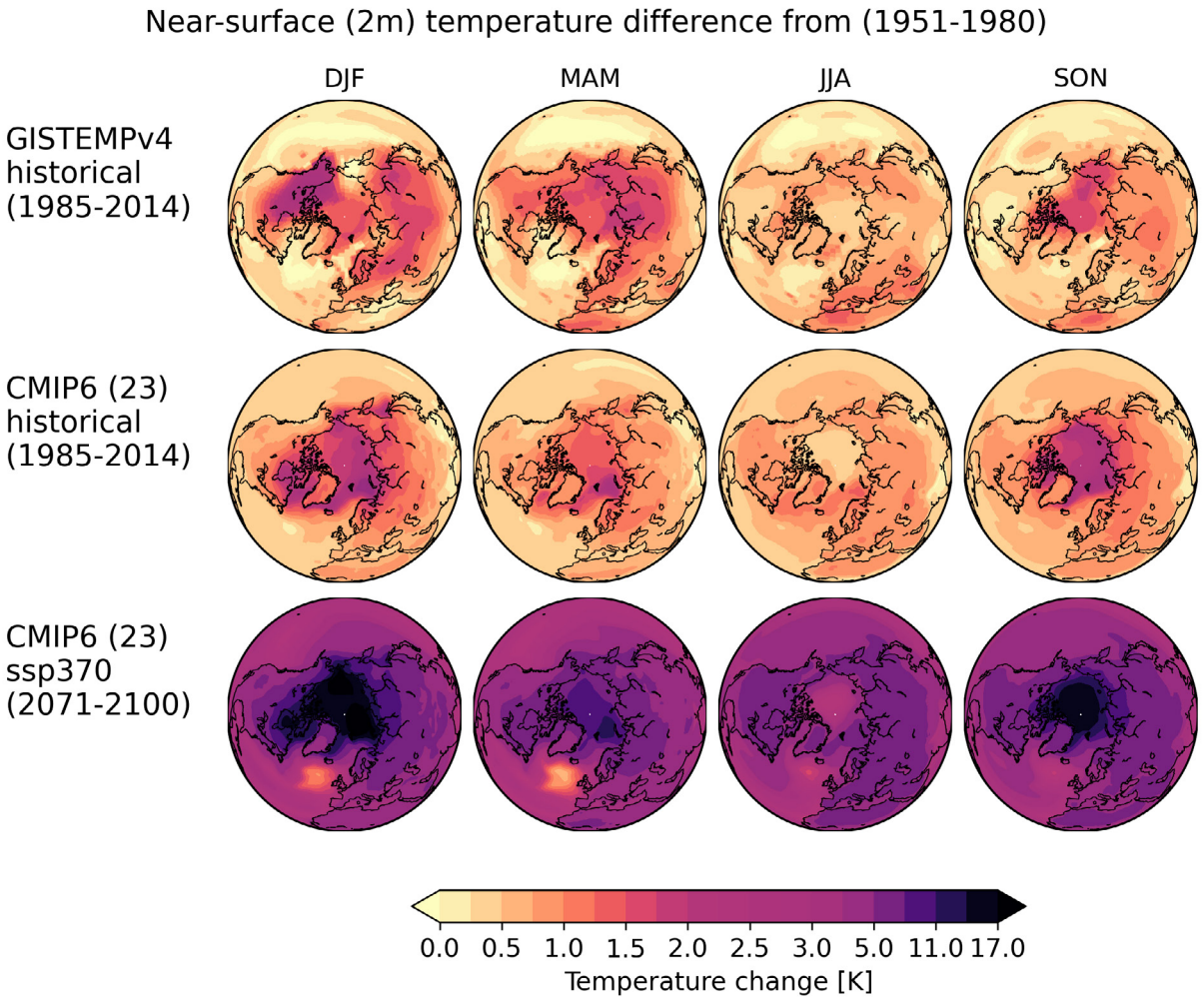

Figure 2: Seasonally averaged anomalies against the baseline (1951–1980) for near-surface (2 m) temperature. The historical (1985–2014) temperature change as found in GISTEMPv4 (upper) and the CMIP6 ensemble mean (middle), and in the projected (2071–2100) temperature change under SSP3-7.0 for CMIP6 (bottom). The numbers in parenthesis after CMIP6 indicate the number of models included in the ensemble mean.

Arctic warming is larger in the CMIP6 ensemble compared to GISTEMPv4. This is especially noticeable in autumn and winter with an AA factor (the ratio of Arctic warming to global warming) of 3.48 (2.24) and 3.75 (2.42) in CMIP6 (GISTEMPv4), respectively. In GISTEMPv4, there is pronounced warming over land, especially in winter and spring (March, April, and May; MAM). In the models, the warming is mostly enhanced over sea ice-covered regions. Interestingly, the region around Svalbard exhibits strong warming compared to the Arctic in winter and spring in both GISTEMPv4 and CMIP6 (see also Table 1).

The AA also shows up clearly in projections of the future climate at the end of the century (here represented by SSP3-7.0; for a description of the SSPs please see Section 3) with an Arctic-averaged winter surface warming of 13°C and as high as 20°C in some regions (Figure 2, bottom panel). In the autumn, the area-averaged surface warming is 10°C for the Arctic and reaches 16°C in some regions. As seen with other warming scenarios (e.g. Graff et al. 2019) AA is less pronounced in an even warmer world than in the present-day climate. The AA factor is slightly reduced in all seasons in SSP3-7.0 at the end of the century compared to the current period in the historical experiment;

Model/Obs	Region	Annual T	Winter T	Annual pr	Winter pr
CMIP6*	Global	**0.26**	**0.27**	**0.38**	**0.37**
	Arctic	**0.70**	**0.92**	**2.96**	3.12*
	Svalbard	**0.78**	1.07*	2.66*	2.89*
ERA5	Global	**0.16**	**0.15**	**0.96**	**1.08**
	Arctic	**0.68**	**0.75**	**1.49**	1.52
	Svalbard	**0.75**	**1.39**	2.02	2.69
MERRA-2	Global	**0.12**	**0.10**	**1.48**	**2.47**
	Arctic	**0.41**	**0.36**	-0.14	-1.34
	Svalbard	**0.52**	**1.12**	0.09	-1.13
NCEP-DOE 2	Global	**0.16**	**0.09**	-	-
	Arctic	**0.88**	**0.92**	-	-
	Svalbard	**0.81**	**1.54**	-	-
GISTEMPv4	Global	**0.16**	**0.13**	-	-
	Arctic	**0.66**	**0.72**	-	-
	Svalbard	**0.69**	**0.94**	-	-
GPCPv2.3	Global	-	-	0.18	**0.60**
	Arctic	-	-	**3.15**	2.30
	Svalbard	-	-	**9.78**	10.58
Svalbard Lufthavn	Svalbard	**1.23**	**2.49**	3.35	4.06
Ny-Ålesund	Svalbard	**0.93**	**2.07**	**10.08**	13.99

Table 1: Linear near-surface temperature (T) trends (°C per decade) and total precipitation (pr) trends (% per decade) for the time period 1980–2014. Trends significant at the 5% level are bold [Mann-Kendall non-parametric test (Mann 1945; Kendall 1975; Hussain and Mahmud 2019]. For CMIP6, the ensemble-mean value of 48 models (see list in Figure 1) is given in bold if more than 75% of the individual models exhibit a significant trend and an * if the CMIP6 ensemble-mean trend is significant, but less than 75% of the individual models exhibit a significant trend.

for example, it is reduced from 3.75 to 3.42 in winter and from 3.48 to 2.83 in autumn (note that for consistency the numbers are based on the 23 models that simulated both the SSP3-7.0 and the historical experiment – but they are very similar to those reported above based on all 48 models). The Arctic summer warming is 0.70°C in the CMIP6 historical (1985–2014) ensemble average and projected to increase by 7°C by the end of the 21st century in SSP3-7.0. Also for summer, the AA factor of 1.32 is slightly reduced in SSP3-7.0, compared to the historical AA factor of 1.51.

In addition to being able to correctly represent the spatial pattern of the recent changes in near-surface temperature, the CMIP6 models must also capture the temporal evolution of these changes over the historical period. In our representation, with the period of 1981–2010 as baseline, it appears, that the CMIP6 models exhibit too strong warming after 1980 (Figure 3, left panels and Table 1). It has been shown that this warming partly compensates for a cooling effect prior to and around the year 1970, imposed by possibly too strong aerosol forcing in the models at that time (Flynn and Mauritsen 2020). Another reason why the models are too warm is that they are unable to properly capture the global warming hiatus between 1998 and 2012, when the annual and global mean surface temperature hardly changed for more than a decade in spite of increasing atmospheric GHG concentrations (Kosaka and Xie 2013; Medhaug et al. 2017). The historical timeseries of annual and global mean near-surface temperature anomalies (Figure 3a) reveal a warming trend of 0.26°C per decade over the 35 years from 1980 to 2014 in the CMIP6 ensemble mean, which is significantly higher than in the reanalysis (Table 1).

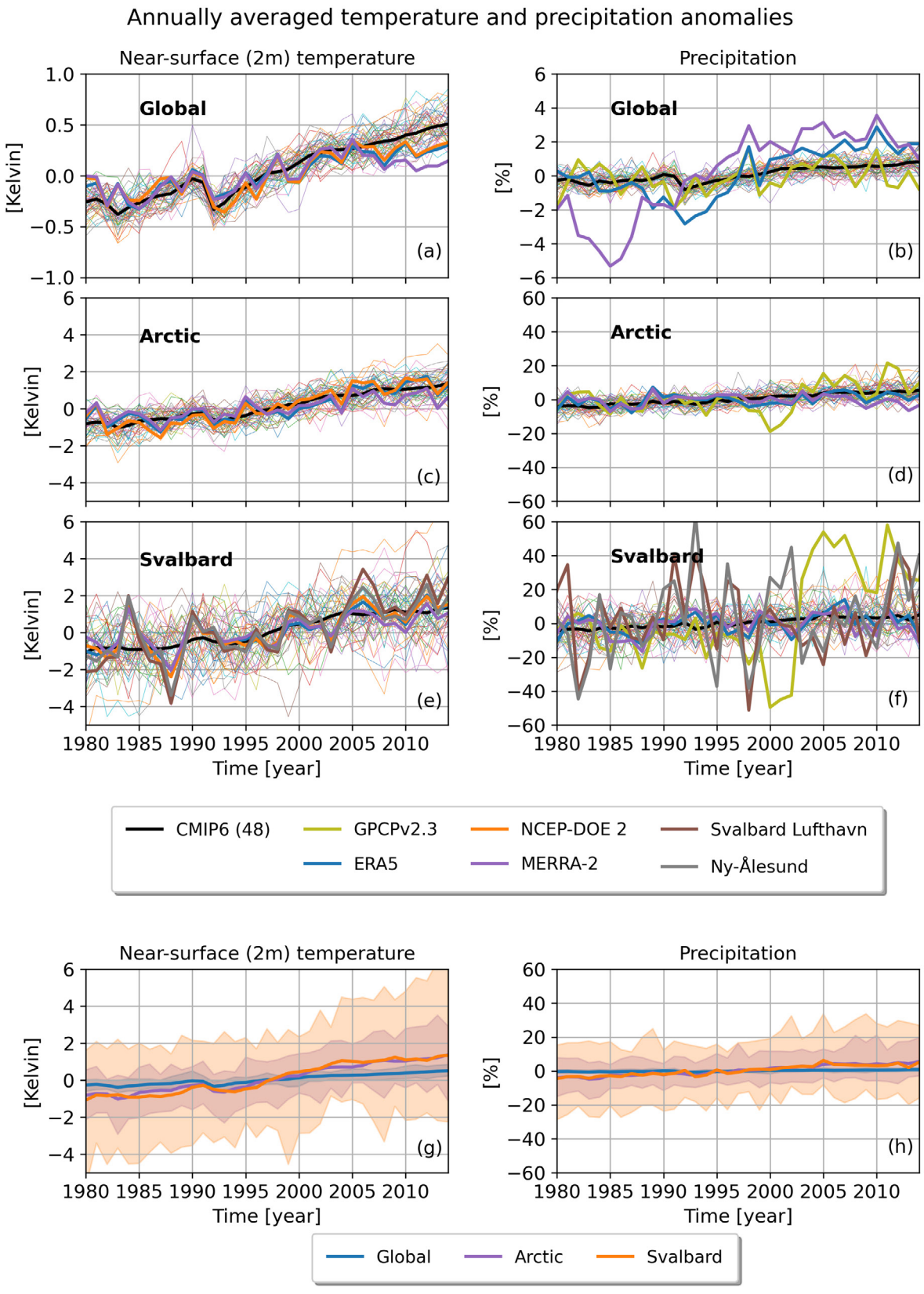

Figure 3: Annually averaged anomalies from the baseline (1981–2010) for near-surface (2 m) temperature (left) and precipitation (right) over the years 1980–2014. The upper 6 panels show the CMIP6 members (thin lines) and the CMIP6 ensemble mean (black line) compared to the reanalysis data: GPCPv2.3 (olive line, only precipitation), ERA5 (blue line), NCEP-DOE 2 (orange line), and MERRA-2 (purple line), in addition to observational records from Svalbard-Lufthavn (brown line), and Ny-Ålesund (grey line). Three regions are considered: global (upper), Arctic (middle) and Svalbard (bottom). The lower 2 panels show the anomalies in temperature (left) and precipitation (right) for the CMIP6 ensem- ble mean (solid line) and the spread (shading) for the global mean (blue), Arctic mean (purple), and Svalbard (orange).

The CMIP6 ensemble-mean temperature evolution in the Arctic and in Svalbard is within the uncertainty of the reanalysis, and AA is clearly visible (Table 1 and Figure 3c,e)[3] with an annual temperature trend (1980–2014) of 0.70°C per decade in the Arctic and 0.78°C per decade in Svalbard. The modelled trends for Svalbard are smaller than the observed temperature trends of 0.93°C per decade in Ny-Ålesund and of 1.23°C per decade in Svalbard Lufthavn (Figure 3e). These trends are higher compared to those reported in Førland et al. (2011): 0.73°C per decade in Ny-Ålesund and 1.04°C per decade in Svalbard Lufthavn for the years 1975–2011. They are clear evidence of the more recent accelerated warming. Updated estimates reveal an even stronger warming trend of 1.66°C per decade over the years 1991 – 2018 in Svalbard Lufthavn (Nordli et al. 2020).

The aforementioned global warming hiatus was in large part dominated by cooling over the Pacific Ocean and over North America towards Eurasia (Kosaka and Xie 2013; Medhaug et al. 2017), and hence is not evident when only the Arctic is considered. The annual mean Arctic warming in CMIP6 is in agreement with ERA5 (Table 1). However, NCEP-DOE 2 exhibits an even stronger warming of 0.88°C per decade. The reanalysis sets agree on a global warming trend of 0.16°C per decade, except for MERRA-2, which exhibits a smaller warming trend of 0.12°C per decade. The smaller annual temperature trend in MERRA-2 is also evident for the Arctic and in Svalbard.

The historical temperature trends for the Arctic and Svalbard are compared for all seasons (Figure 4a). 63% of the CMIP6 models exhibit a stronger temperature trend in winter in Svalbard compared to the Arctic. However, only 13% of the individual models exhibit a statistically significant warming trend at the 5% level (Mann-Kendall non-parametric test; Mann 1945; Kendall 1975; Hussain and Mahmud 2019)[4]. Importantly, the ensemble mean value of 0.92°C per decade for the Arctic and 1.07°C per decade for Svalbard is significant even at the 1% level. The stronger temperature trend in Svalbard compared to the Arctic in the CMIP6 ensemble mean is present for all seasons, except autumn, with a 0.09°C per decade (annual) and a 0.15°C per decade (winter) enhanced warming trend. Of the reanalysis sets, only MERRA-2 exhibits a significantly stronger warming trend in Svalbard compared to the Arctic with a 0.40°C per decade and 0.70°C per decade warmer trend for the annual and winter mean respectively.

2.2. Precipitation

In conjunction with the temperature increase, the total precipitation increases on a global scale as well as in the Arctic (Figure 3, right panels and Table 1). The historical CMIP6 timeseries of annual mean area-averaged total precipitation exhibits a significant increase of 0.37% per decade in the global mean over the years 1980–2014 compared to 3.12% per decade and 2.89% per decade in the Arctic and in Svalbard, respectively. The CMIP6 ensemble mean and the reanalysis GPCPv2.3 experience a significantly larger trend in the Arctic and Svalbard compared to the global mean. The CMIP6 ensemble mean demonstrates a wetter trend of 2.61% per decade for the Arctic and 2.30% per decade in Svalbard, compared to the global annual mean.

The hydrological cycle has intensified in response to global warming, and consequently the atmospheric moisture transport to the Arctic has increased (Held and Soden 2006; Serreze et al. 2012; Hartmann et al. 2013; Hanssen-Bauer et al. 2019). In addition, amplified temporal fluctuations and the changes in the atmospheric circulation in the mid-latitudes in response to the warming could further enhance the moisture transport into the Arctic (Zhang et al. 2008). The precipitation timeseries (Figure 3, right panels) reveal great disagreement among the CMIP6 models as well as among the reanalyses, reflecting that the hydrological cycle is challenging to model. Precipitation occurs in large part on sub-grid scales and hence is parameterized in climate models. In contrast to temperature, which is a more direct response of radiation, precipitation

3 Please note the different y-axis
4 All statistically significant trends in this report are significant at the 5% level, using the Mann-Kendall non-parametric test, if not stated differently

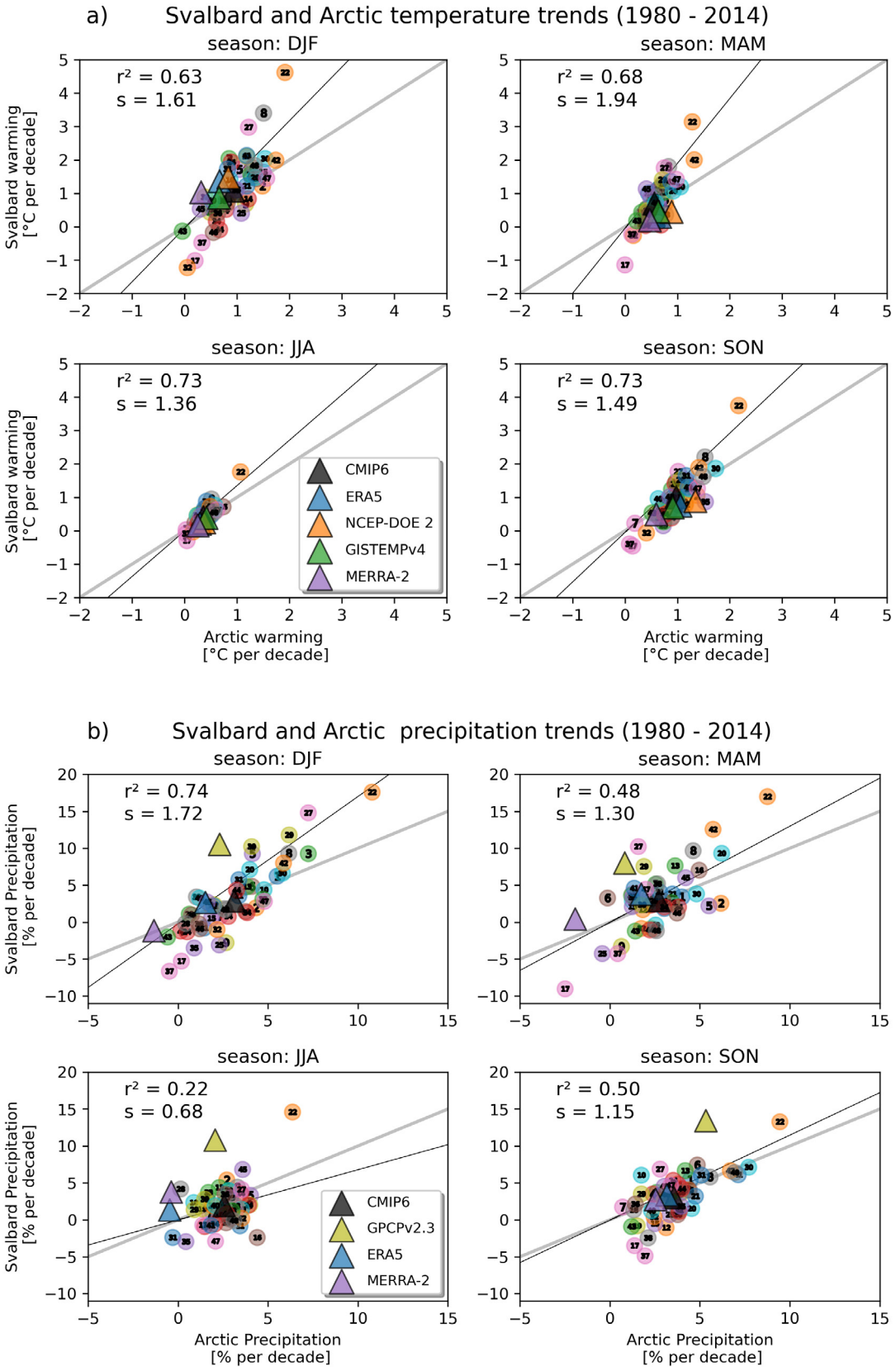

Figure 4: Near-surface (2 m) temperature (upper 4 panels) and precipitation trends (lower 4 panels) for the Arctic and Svalbard for all seasons. All panels show 48 ESM historical simulations (coloured dots) and the CMIP6 ensemble mean (black triangle) and are compared to similar trends in reanalysis and observational datasets: ERA5 (blue triangle), NCEP-DOE 2 (orange triangle), GISTEMPv4 (green triangle), MERRA-2 (purple triangle), and GPCPv2.3 (olive triangle). Also indicated is the 1:1 agreement (grey line) and the linear regression of the CMIP6 model results (black line).

involves various nonlinear interactions of processes such as evaporation, convection, cloud formation, and temperature and pressure fluctuations. In addition, the reanalyses are sensitive to a lack of good observations of precipitation (Zhang et al. 2013). Further, in response to global warming, it is particularly hard to obtain realistic treatment of processes such as degradation of permafrost, Arctic greening and reduction of plant transpiration which can act to intensify the hydrological cycle in addition to the atmospheric circulation changes (Zhang et al. 2013).

The historical precipitation trends for the Arctic and Svalbard are compared for all seasons (Figure 4b, also see Table 1). In the Arctic, 44% of the individual models exhibit a statistically significant increased precipitation trend during winter, and as many as 82% do so during autumn. The CMIP6 ensemble mean exhibits a significant increase in precipitation of 3.12% per decade (winter) and 3.56% per decade (autumn) for the Arctic. In Svalbard, the percentage of individual models exhibiting a significant increasing precipitation trend is reduced to 29% (winter) and 23% (autumn). However, the CMIP6 ensemble mean exhibits a significant increased precipitation trend of 2.89% per decade (winter) and 3.02% per decade (autumn) in Svalbard.

The CMIP6 ensemble mean shows a significantly larger annual precipitation trend in the Arctic than in Svalbard, being 0.23% wetter per decade. This is also evident in the autumn where the Arctic precipitation trend is 0.74% per decade wetter compared to Svalbard. The observed precipitation trends from GPCPv2.3 are wetter in Svalbard compared to the Arctic in summer (7.89% per decade) and autumn (8.35% per decade) and also in the annual mean (5.70% per decade). None of the reanalyses exhibit significant differences in the precipitation trends in the Arctic and Svalbard.

2.3. Sea ice

Sea-ice loss and changes in the associated sea-ice albedo feedback is an important factor contributing to AA (Cohen et al. 2020). The bright sea-ice surface efficiently reflects solar radiation during spring and summer. As the sea ice melts, this bright reflecting surface is replaced by a dark absorbing ocean. The absorbed heat is returned to the cold atmosphere during autumn and spring (Serreze et al. 2009) causing extensive warming and further sea-ice loss — creating a positive feedback. This feedback loop is one of the main reasons why the Arctic is warming so fast compared to the rest of the world (Pithan and Mauritsen 2014; Kim et al. 2019). Liang et al. (2020) find that in climate models, as much as 21% of the Arctic-averaged near-surface winter temperature are accounted for by the Arctic sea-ice concentration-driven variance over the years 1979–2014.

In fact, the amplified warming in the Arctic causes sea ice melt at a pace greater than that simulated by the climate models (Cohen et al. 2014, 2020). The Arctic experiences sea ice loss across all seasons (Stroeve and Notz 2018) with the greatest loss in the autumn (Figure 5, right columns). 44 models participating in CMIP6 exhibit a declining trend in the September sea-ice extent of $(-0.7 \pm 0.06) \times 10^6$ km^2 per decade over the years 1979–2014, while the observed trend is even larger $(-0.82 \pm 0.18) \times 10^6$ km^2 per decade (Shu et al. 2020). In this report, we consider 30 of the 48 models listed in Figure 1, and Arctic sea ice is defined as the Northern Hemisphere total sea-ice extent.

On average, the sea-ice extent in CMIP6 is too large compared to observations and all the reanalyses. This is especially evident in spring (MAM, Figure 5a). 90% of the individual models exhibit a significant decline in sea-ice extent with an ensemble-mean decadal trend over the years 1980–2014 of -0.36×10^6 km^2 for spring (MAM) and -0.57×10^6 km^2 for autumn (SON) (Figure 5a,b). The discrepancy between the autumn trend of -0.57×10^6 km^2 per decade reported in this study and the $(-0.7 \pm 0.06) \times 10^6$ km^2 per decade listed above, is due to different averaging periods (SON vs. September only) and a different number of models (30 vs. 44). Of the observational dataset (HadISST) and reanalyses (ERA5 and MERRA-2), only ERA5 exhibit a larger decadal decline in Arctic sea-ice extent in the autumn (-0.69×10^6 km^2), while the corresponding value for HadISST is -0.55×10^6 km^2 and in agreement with the CMIP6 ensemble mean value.

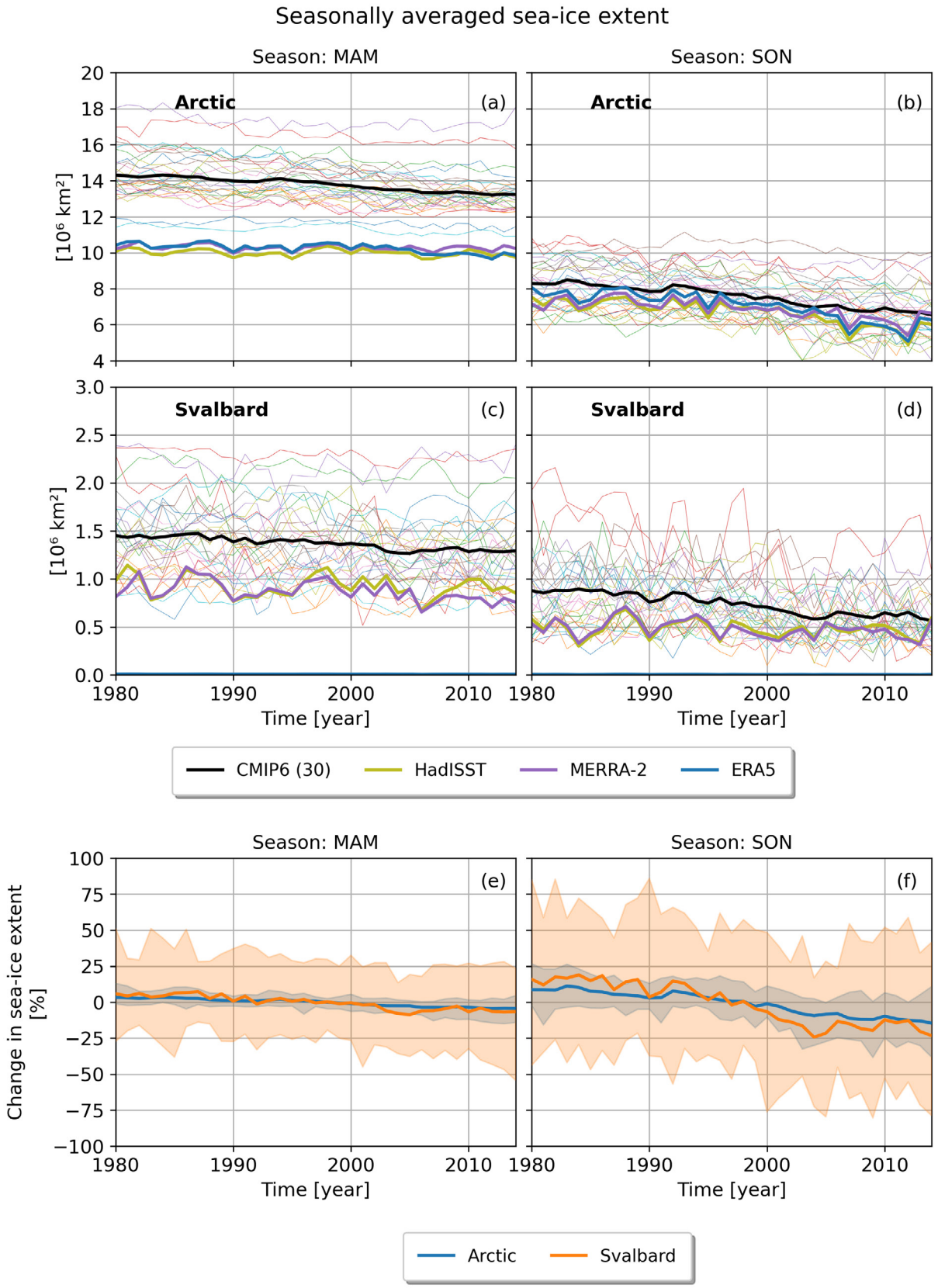

Figure 5: Sea-ice extent in the MAM season and the SON season for the years 1980–2014. The upper 4 panels show the CMIP6 members (thin lines) and the CMIP6 ensemble mean (black line) compared to the reanalysis data: HadISST (olive line), MERRA-2 (purple line), and ERA5 (blue line). Two regions are considered: Arctic (upper) and Svalbard (bottom). The lower 2 panels show the anomalies in sea-ice extent from the baseline (1981–2010) as a percentage change for the MAM season (left) and the SON season (right) for the CMIP6 ensemble mean (solid line) and the spread (shading) for the Northern Hemisphere (blue) and Svalbard (orange).

In Svalbard, 43% and 77% of the individual models exhibit a significant decline in sea-ice extent in spring (MAM) and autumn (SON) (Figure 5c,d). One model (CNRM-CM6-1) exhibits a significant increasing trend in sea-ice extent in spring. The CMIP6 ensemble-mean decadal trend is -0.06×10^6 km^2 for spring (MAM) and -0.10×10^6 km^2 for autumn (SON) (Figure 5c,d).

When comparing the decadal decline in sea-ice extent for Arctic and the Svalbard region, we consider the percentage changes (Figure 5, bottom row). In CMIP6, the sea-ice extent declines faster in the region around Svalbard, compared to the Arctic, and the difference is most prominent in the autumn with a sea-ice loss of -13.7% per decade in Svalbard, compared to -7.5% per decade in the Arctic. 37% of the individual models exhibit a significantly more negative trend in the region around Svalbard compared to the Arctic. The CMIP6 ensemble mean exhibits a significantly faster decline of -6.20% in sea-ice extent around Svalbard compared to the Arctic as a whole.

3. Future projections of Arctic climate

To study how temperature, precipitation, and sea-ice extent may change over the upcoming 80 years, we consider results from four CMIP6 climate projections known as "shared socioeconomic pathways" (SSPs; O'Neill et al. 2016): **SSP1-2.6**, the "best-case" scenario where mitigation and adaptation challenges are low and the radiative forcing due to anthropogenic activities reaches 2.6 W m^{-2} by the end of the 21st century; **SSP2-4.5**, a mid-range scenario with respect to both mitigation and adaptation and with the radiative forcing reaching 4.5 W m^{-2} in 2100; **SSP3-7.0**, a future with high mitigation and adaptation challenges and high radiative forcing of 7.0 W m^{-2} in 2100; **SSP5-8.5**, the "worst-case" scenario with high mitigation challenges, low adaptation challenges, and the radiative forcing exceeding 8.5 W m^{-2} by 2100.

We consider results from the SSPs alongside results from the historical runs using data from the 23 CMIP6 models that provide the necessary data from all simulations.

3.1. Near-surface temperature

The annually and globally averaged near-surface temperature increases by 0.89°C over the historical period (1900–2014; Figure 6). The temperature continues to increase in the future, both in terms of the global mean (Figure 6, upper left) and for the Arctic (middle left) and Svalbard regions (bottom left). The temperature increase is however substantially larger in the high-latitude regions (note top panel has different y-axis). The scenarios start diverging around 2040, and by 2100, there is considerable spread between the best- and worst-case scenarios, with the global-mean ensemble-mean warming over the last 10 years (2091–2100, compared to the baseline years 1850–1879) ranging from 1.97°C (SSP1-2.6) to 4.85°C (SSP5-8.5), whereas the CMIP6 ensemble-mean warming for the Arctic and Svalbard ranges from 6.80°C to 18.20°C and 7.37°C to 15.35°C, respectively.

The enhanced winter warming in the Arctic and Svalbard is evident in all scenarios (Figure 6). Interestingly, by 2100 Svalbard experiences greater warming compared to Arctic for the historical period and the two mildest future scenarios (SSP1-2.6 and SSP2-4.5). However, for the two warmest scenarios (SSP3-7.0 and SSP5-8.5), the Arctic experiences greater warming. The reason for this shift is probably the lack of sea-ice feedback as all the sea ice in the region around Svalbard has melted by 2100 under the warmest scenarios (Figure 7, right). However, only the winter warming for the SSP5-8.5 scenario is significantly warmer in the Arctic than in Svalbard (Mann-Whitney U Test, $p = 0.007$, Mann and Whitney 1947).

There is vast inter-model spread; for instance, for Svalbard the winter warming over the years 2091–2100 (compared to the baseline years 1850–1879) for SSP5-8.5 ranges from 9.70°C to 25.91°C (see

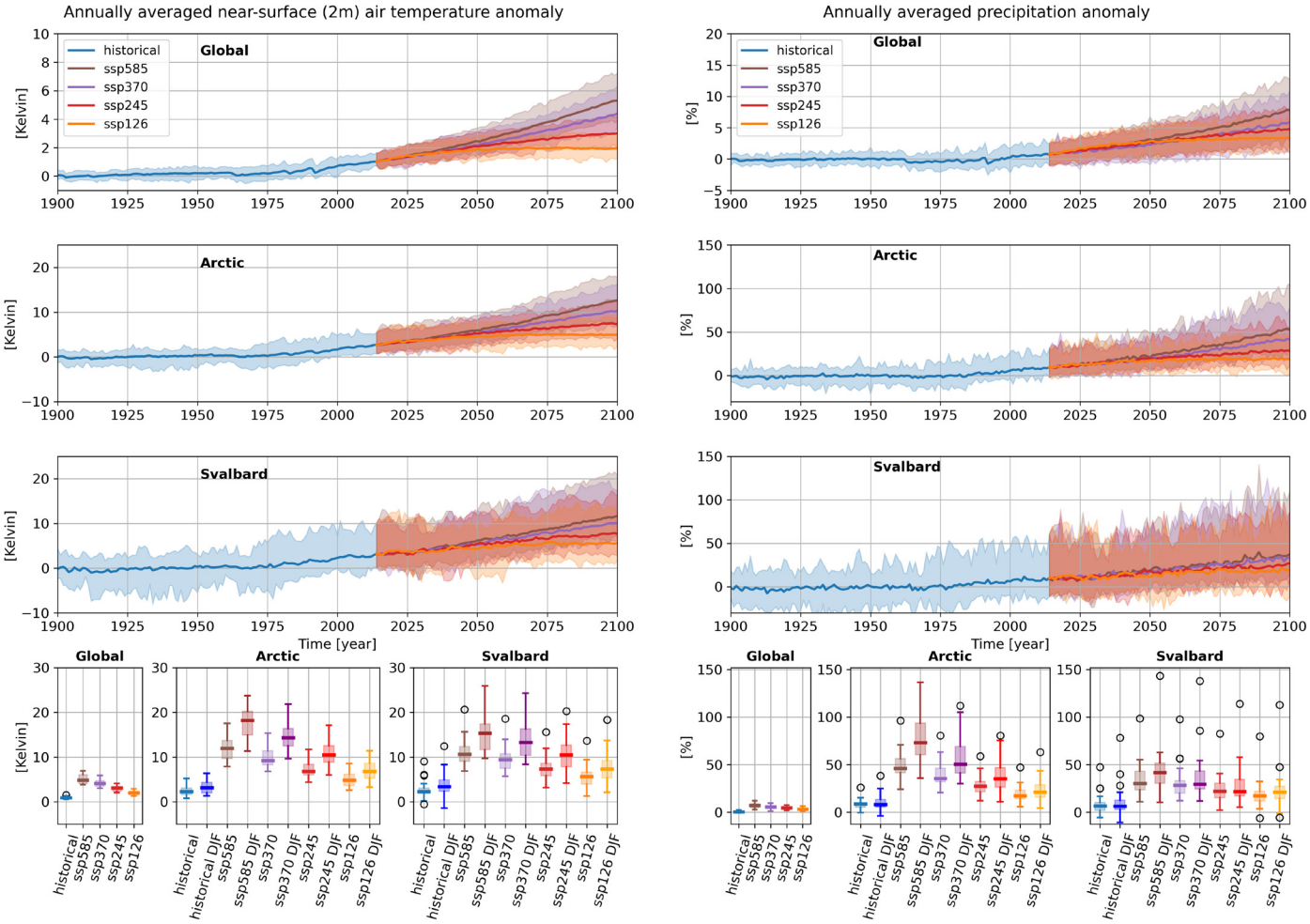

Figure 6: Annual-mean anomalies of near-surface (2 m) temperature (left column) and precipitation (right column) from the historical runs (1900–2014) and future projections (2015–2100) for three regions: the globe (upper row), the Arctic (second row), and Svalbard (third row). The anomalies are taken with the years 1850–1879 as a baseline. The upper four panels show the time evolution of the historical run (blue), SSP5-8.5 (brown), SSP3-7.0 (purple), SSP2-4.5 (red), and SSP1-2.6 (orange) for the CMIP6 ensemble mean (solid lines) and the spread (shading). The bottom row shows the box plots of area-averaged anomalies % of sea-ice extent from the historical runs and future projections for annual-mean global values, global-mean, and DJF values for the Arctic and global-mean and DJF values for Svalbard averaged over 2091–2100 (the last decade shown in the upper four panels). The horizontal line within the box shows the median value, the boxes show the interquartile range, the whiskers extend to the smallest and largest values that are not outliers, and the open circles show the outliers. For the Arctic and Svalbard, plots for DJF are shown alongside.

brown shading in Figure 6). The inter-model spread increases as we zoom in on smaller regions, with Svalbard having the largest spread; the spread is moreover larger when only considering the winter season (Figure 6, bottom panel). Presumably, the inter-model spread of area-averaged quantities is smaller for the larger domain because more data points are included. For smaller domains, the average could be more sensitive to whether values in the tails of the distributions fall within the domain or not. For the Svalbard region, the position of the marginal ice zone, which can vary between the models, exerts a large influence on temperature, potentially causing large inter-model temperature spread. Similarly, the inter-model spread could be larger for the winter means than the annual means because fewer data (25%) are used when computing the winter means. However, the winter season is also characterised by more variability with, for instance, the North Atlantic storm track being more vigorous and also more tilted toward the pole compared to during summer (Shaw et al. 2016). Further investigation is warranted to understand this properly.

3.2. Precipitation

While the precipitation trend seems to be rather weak (0.5% increase) over the historical period, it clearly increases in the future climates. As with

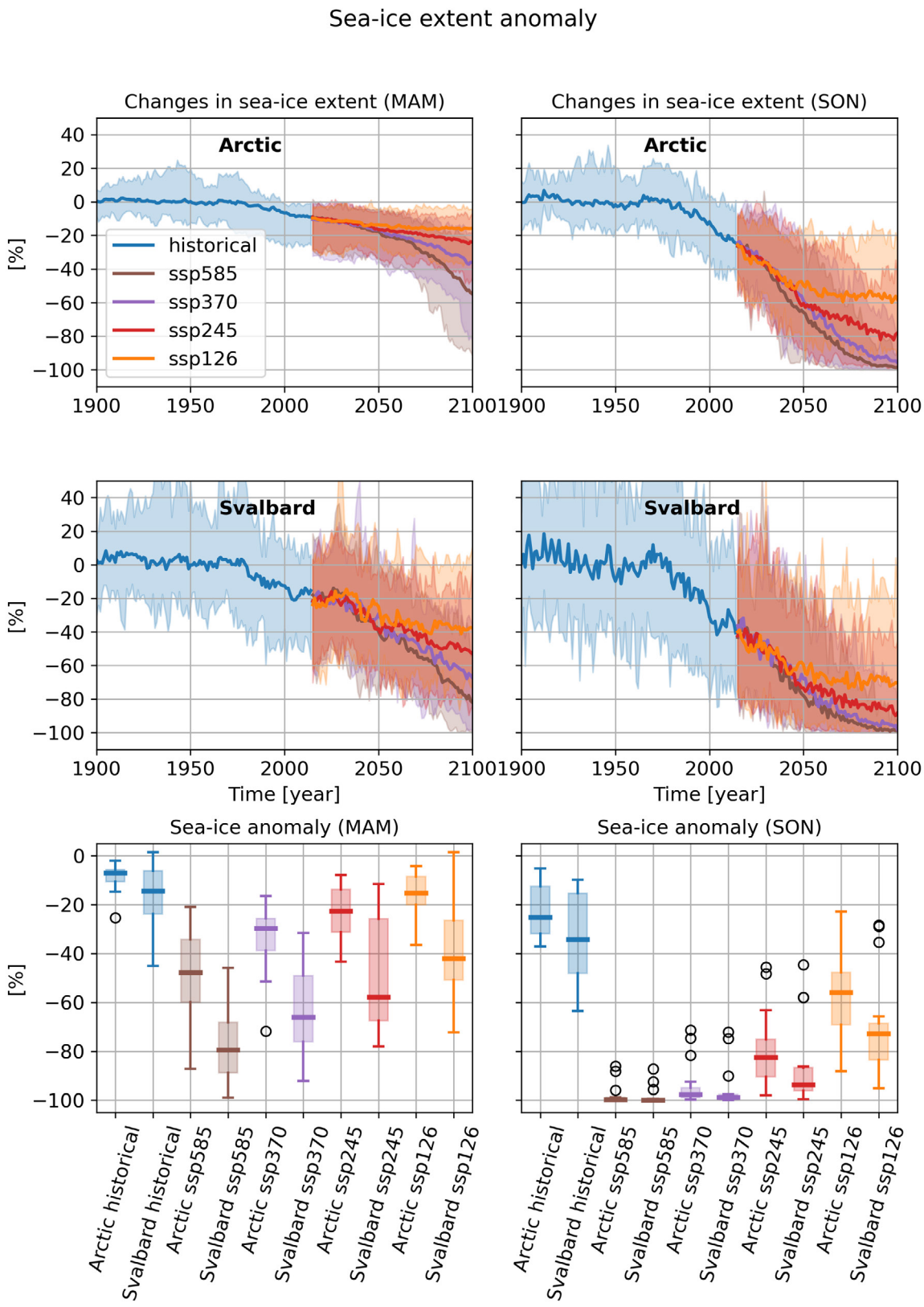

Figure 7: Annual-mean anomalies of the sea-ice extent from the historical runs (1900–2014) and future projections (years 2015–2100) for the Arctic and Svalbard regions for MAM (left column) and SON (right column). The anomalies are taken with the years 1850–1879 as a baseline. The upper four panels show the time evolution of the sea-ice extent anomalies for the historical (blue), SSP5-8.5 (brown), SSP3-7.0 (purple), SSP2-4.5 (red), and SSP1-2.6 (orange) timeseries for the CMIP6 ensemble mean (solid lines) and the spread (shading) for the Arctic (top row) and Svalbard (middle row) regions. The bottom row shows box plots of area-averaged anomalies of sea-ice extent from the historical runs and future projections for the Arctic and Svalbard averaged over 2091–2100 (the last decade shown in the upper four panels). The horizontal line within the box shows the median value, the boxes show the interquartile range, the whiskers extend to the smallest and largest values that are not outliers, and the open circles show the outliers.

temperature, the increase is larger for the Arctic and Svalbard regions than it is globally (note the different y-axis). The global-mean ensemble-mean change in precipitation by year 2100 ranges from 3% for SSP1-2.6 to 7% for SSP5-8.5, whereas the corresponding numbers for the Arctic and Svalbard are 21% to 73% and 21% to 42%, respectively.

As with temperature, the inter-model spread is largest for Svalbard and smallest for the global mean; the spread is also larger when considering just the winter months compared to the whole year. Interestingly, the inter-scenario spread, that is, the spread between the different SSPs, is larger for the Arctic than for Svalbard. This could indicate that for Svalbard, the change in precipitation by 2100 depends less on the chosen scenario than it does for the Arctic as a whole. The ensemble-mean precipitation reaches lower values under SSP5-8.5 for Svalbard than for the Arctic, but higher values for SSP1-2.6, suggesting that Svalbard could experience a larger increase in precipitation than the Arctic under the best-case scenario, while the roles could be reversed under the worst-case scenario. However, only the two warmest and wettest scenarios (SSP3-7.0 and SSP5-8.5) show a significantly larger increase in annual and winter precipitation in the Arctic compared to Svalbard (Mann-Whitney U Test, $p < 0.001$, Mann and Whitney 1947).

3.3. Sea ice

As expected, the sea-ice extent decreases with time over the historical period and continues to decrease with future warming, both when considering the Arctic (i.e. the Northern Hemisphere sea-ice extent), and when narrowing down to the Svalbard region (Figure 7). The changes are largest in the scenarios with the strongest warming. During spring, the sea-ice extent is projected to decrease by 48% for the worst-case scenario (SSP5-8.5) and 15% for the best-case scenario (SSP1-2.6) for the Arctic and by 79% for the worst-case scenario and 42% for the best-case scenario for Svalbard by 2100.

Ice-free conditions are reached under both the worst-case scenario and SSP3-7.0 during autumn, whereas for the best-case scenario, the sea-ice extent decreases by 56% for the Arctic and 73% for Svalbard. There is large inter-model variability both during the historical period and in the future projections. The variability however decreases as the sea-ice extent decreases, and is very low by the end of the 21st century (Figure 7, bottom right panel).

4. Concluding remarks

Our study shows that compared to the temporal evolution in the global mean of selected climate variables, Svalbard and the Arctic undergo similar and significantly larger changes in response to projected future climate change and to the warming that has occurred over the last few decades. Thus, we find that Svalbard is well-suited as an observational supersite for the Arctic. There are however important differences:

- The Svalbard region displays an even stronger warming trend than the Arctic for the historical period (1980–2014) and for the two mildest future scenarios (SSP1-2.6 and SSP2-4.5). However, the winter warming for the worst case scenario (SSP5-8.5) is significantly warmer in the Arctic than in Svalbard.
- In the future, the Arctic experiences a significantly larger increase in annual and winter precipitation compared to Svalbard for the two warmest and wettest (SSP3-7.0 and SSP5-8.5) climate projection scenarios.
- Over the more recent historical period (1980–2014), the sea ice melts faster in the region around Svalbard than in the Arctic.

5. Connections and synergies with other SESS report chapters

Good and accurate observations are of critical importance for Earth System Modelling. Observations are needed in order to improve our understanding of the state of the Earth system and distribution of different quantities, processes, and interactions. This knowledge is utilised in the models to make sure that the Earth system is represented as realistically as possible. Observations are also needed to validate the model output and help us identify quantities and processes that are well-represented or that need further improvement. The work presented here therefore has synergies with several other chapters from SESS reports, for instance, in relation to observations of snow cover and sea ice ("Long-term monitoring of landfast sea-ice extent and thickness in Kongsfjorden, and related applications (FastIce)" by Gerland et al. 2020; "Long-term variability of terrestrial-snow and sea-ice cover extent in Svalbard (SvalSCESIA)" by Killie et al. 2021), cloud condensation nuclei ("Multidisciplinary research on biogenically driven new particle formation in Svalbard (SVALBAEROSOL)" by Sipilä et al. 2020), atmospheric black carbon ("Atmospheric black carbon in Svalbard (ABC Svalbard)" by Gilardoni et al. 2020) and Arctic haze ("Arctic haze in a climate changing world (HAZECLIC)" by Traversi et al. 2021).

6. Unanswered questions

Some of the mechanisms contributing to Svalbard/Arctic differences in temperature, precipitation, and sea-ice extent need further investigation and are listed below.

Svalbard lies in the vicinity of the North Atlantic transport pathways, which bring heat, moisture, and matter to the Arctic by both atmospheric and oceanic processes and which connect the Arctic to the larger-scale circulation. Hence, transport changes due to anthropogenic forcing may cause a greater impact in Svalbard compared to the Arctic as a whole, and/or the timescales of impact may differ greatly, but that needs further investigation.

The West Spitsbergen Current (WSC) brings warm and saline Atlantic water into the Arctic and connects the Arctic and the world oceans. The Arctic near-surface temperature and sea-ice extent can be mediated by this inflow, both in the present climate (Chylek et al. 2009; Mahajan et al. 2011) and in projections of future climate change (Nummelin et al. 2017). In our study we found that over the more recent historical period (1980–2014), the sea ice melts faster in the region around Svalbard than in the Arctic. A reduction in sea-ice extent is intimately linked to temperature changes, and our results show that the Svalbard region displays an even stronger warming trend than the Arctic for the historical period (1980–2014). How these reported changes between Svalbard and the Arctic are linked to the ocean transport needs further investigation.

North Atlantic storms typically travel poleward and eastward from the east coast of the U.S. toward the Barents Sea. The storms bring warm moist air from lower to higher latitudes, and are an important contributor to the atmospheric poleward heat transport. Changes in the pathways of these storms can change this transport and therefore have the potential to affect the Arctic as a whole and perhaps even more so Svalbard, as it is situated in the north-eastern edge of the storm track and is greatly affected by the details of the paths taken by the storms. In addition, the discrepancy between the observed storm tracks and those simulated by the models has implications for atmospheric poleward heat transport, precipitation, and strong winds. It can even be a major cause of why models fail to fully capture observed climate change in Svalbard and the Arctic as a whole.

In order to quantify the most important drivers for climate change in Svalbard and for the Arctic

as a whole, it remains an open question how one can quantify the contributions from the large-scale atmospheric circulation changes, such as shifts in the storm tracks, changes in the oceanic heat transport into the Arctic, and how to disentangle such contributions from the various feedbacks amplifying the warming. Likewise, it is still difficult to differentiate between large-scale drivers and more local changes (Isaksen et al. 2016). How confident can we be of modelled attribution of climate change when interpreting locally observed timeseries of physical and biogeochemical variables?

In this study, we have considered the Arctic as a whole. Further investigation is needed to understand for which parts of the Arctic the Svalbard region can act as a supersite and can be used as an early warning platform.

7. Recommendations for the future

The climate models are highly complex numerical models, fed with initial conditions (for instance the current state of the Earth system or perturbed states) to simulate, for instance, the historical period or to project future scenarios. Due to the chaotic nature of the system, understanding the data produced by the models is challenging. Although often very impressive in their complexity, the models are imperfect and not always able to accurately reproduce all aspects of the Earth system. To be able to tell where the models fail and where they succeed, we need to understand why they act as they do. In particular, we need to make sure that the correctness of future projections made by these models rest on our understanding of the system. To achieve that, observations and process understanding are of crucial importance. For instance, incorrect atmospheric and oceanic transports of energy into the Arctic have large impacts on the rate of warming. The model community can benefit not only from the great observational data collected on and in the regions around Svalbard, but also from process understanding of experimentalists and observationalists. Likewise, the experimentalists and observationalists can benefit greatly by interacting more with the modelling community and learn from their perspectives – "the purpose of models is not to fit the data, but to sharpen the questions" (Karlin 1983).

Predicting and characterising climate change in Svalbard will be an increasingly important issue in the 21st century as the changes in near-surface air temperature, precipitation and sea-ice extent seem to occur at an extremely high pace in Svalbard, even higher than in the rest of the Arctic. It is equally important to understand and explain what mechanisms are causing the differences between the observed and modelled climate changes. A closer collaboration between experimentalists, observationalists, and the model community has the potential to improve the understanding of Arctic climate change for the science community, stakeholders, and the public at large. Svalbard Integrated Arctic Earth Observing System (SIOS) is in a unique position to facilitate such a collaboration.

To address the knowledge gaps identified above, we recommend that SIOS supports and initiates consolidated efforts to strengthen the relevant research infrastructure components, both within and outside SIOS. Such efforts will enable other Norwegian and Arctic research institutions to pursue urgently needed research projects in the area of Arctic climate change.

Specifically we recommend:

Supporting efficient data mining and harmonisation efforts, beyond metadata catalogues, which allow the construction and monitoring of energy budgets and energy flux trends in the larger Svalbard region and the Arctic as a whole. Energy flux estimates in the atmosphere, the ocean, and the cryosphere require broad efforts in data assembly and quality assurance, including efforts to seek feedback on usability and usefulness of datasets from model users.

Cooperating with the Norwegian national ESM infrastructure INES to build the modelling tools

needed to integrate the new SIOS data and explore how comparisons between data from models and observations can provide meaningful answers to questions related to Arctic amplification, abrupt changes, and climate feedbacks.

Fostering e-science tools (and education) so that young scientists working in the area of Arctic climate science are able to efficiently analyse results from model ensembles, such as CMIP6.

Initiating and strengthening the collaboration with existing pan-Arctic research initiatives and institutions to assemble temporal trends of physical climate variables in all spheres, along with those of biogeochemical tracers of system changes (methane, aerosols, carbon isotopes, and water isotopes).

Identifying and documenting the most efficient international means of cooperation to foster joint understanding of forthcoming Arctic climate changes, possible abrupt climate transitions, and the drivers for such changes.

8. Data availability

All original data used in this report are openly accessible via the links in table 2. All code used for the analysis can be obtained from the corresponding author upon request.

Table 2: Data sets used in this report

Data set	Time period	Region	Data info, providers and access
CMIP6	1850–2100	Global	All CMIP6 data used in this report are made publicly available in a standardised format and are free to download and accessible from any of the portals listed under "model output access" at https://pcmdi.llnl.gov/CMIP6/
ERA5	1979–Present	Global	ERA5 data are provided by the Copernicus Climate Change Service (C3S), from the Copernicus Climate Change Service Climate Data Store (CDS): https://www.ecmwf.int/en/forecasts/datasets/reanalysis-datasets/era5
MERRA-2	1980–Present	Global	MERRA-2 data are provided by NASA, and made available at MDISC, managed by the NASA Goddard Earth Sciences (GES) Data and Information Services Center (DISC): https://gmao.gsfc.nasa.gov/reanalysis/MERRA-2/docs/
GISTEMPv4	1880–Present (baseline 1951–1980)	Global	GISTEMPv4 data are provided by the NOAA/OAR/ESRL PSL, from their website at https://data.giss.nasa.gov/gistemp/
HadiSST v1.1	1871–Present	Global	HadiSST data can be accessed through the Met Office Hadley Centre at http://badc.nerc.ac.uk/view/badc.nerc.ac.uk ATOM dataent_hadisst
GPCPv2.3	1979–Present	Global	GPCP Precipitation data are provided by the NOAA/OAR/ESRL PSL, from their website at https://psl.noaa.gov/
NCEP-DOE 2	1979–Present	Global	NCEP-DOE reanalysis 2 data are provided by National Centers for Environmental Prediction/National Weather Service/NOAA/, from the Research Data Archive at the National Center for Atmospheric Research, Computational and Information Systems Laboratory: https://doi.org/10.5065/KVQZ-YJ93.

Acknowledgements

The authors thank the Editorial Board, Christiane Hübner, and two anonymous reviewers for their comprehensive and insightful comments, which have led to the improved presentation of this report. This work was supported by the European Framework Programme Horizon 2020 project CRESCENDO (Coordinated Research in Earth Systems and Climate: Experiments, Knowledge, Dissemination and Outreach, grant agreement no. 641816), the Research Council of Norway through project number 291644, Svalbard Integrated Arctic Earth Observing System – Knowledge Centre,operational phase, INES (270061) and KeyCLIM (295046). High performance computing and storage resources were provided by the Norwegian infrastructure for computational science UNINETT Sigma2 (through projects NN2345K, NN9560K, NN9252K, NS2345K, NS9560K, NS9252K, and NS9034K).

References

Bintanja R, Selten F (2014) Future increases in Arctic precipitation linked to local evaporation and sea- ice retreat. Nature 509(7501):479–482, http://doi.org/10.1038/nature13259

Chylek P, Folland CK, Lesins G, Dubey MK, Wang M (2009) Arctic air temperature change amplification and the Atlantic Multidecadal Oscillation. Geophys Res Lett 36(14):L14801, https://doi.org/10.1029/ 2009GL038777

Cohen J, Screen JA, Furtado JC, Barlow M, Whittleston D, Coumou D, Francis J, Dethloff K, Entekhabi D, Overland J, Jones J (2014) Recent Arctic amplification and extreme mid-latitude weather. Nat Geoscience 7(9):627–637, https://doi.org/10.1038/ngeo2234

Cohen J, Zhang X, Francis J, Jung T, Kwok R, Overland J, Ballinger TJ, Bhatt US, Chen HW, Coumou D, Feldstein S, Gu H, Handorf D, Henderson G, Ionita M, Kretschmer M, Laliberte F, Lee S, Linderholm HW, Maslowski W, Peings Y, Pfeiffer K, Rigor I, Semmler T, Stroeve J, Taylor PC, Vavrus S, Vihma T, Wang S, Wendischa M, Wu Y, Yoon J (2020) Divergent consensuses on Arctic amplification influence on midlatitude severe winter weather. Nat Clim Change 10:20–29, https://doi.org/10.1038/s41558-019-0662-y

Dahlke S, Hughes NE, Wagner PM, Gerland S, Wawrzyniak T, Ivanov B, Maturilli M (2020) The observed recent surface air temperature development across Svalbard and concurring footprints in local sea ice cover. Int J Climatol 40(12):5246–5265, https://doi.org/10.1002/joc.6517

Ding M, Wang S, Sun W (2018) Decadal Climate Change in Ny-Ålesund, Svalbard, A Representative Area of the Arctic. Condensed Matter 3(2):12, https://doi.org/10.3390/condmat3020012

Doyle JG, Lesins G, Thackray CP, Perro C, Nott GJ, Duck TJ, Damoah R, Drummond JR (2011) Water vapor intrusions into the High Arctic during winter. Geophys Res Lett 38(12):L12806, https://doi.org/10.1029/2011GL047493

Eyring V, Bony S, Meehl GA, Senior CA, Stevens B, Stouffer RJ, Taylor KE (2016) Overview of the Coupled Model Intercomparison Project Phase 6 (CMIP6) experimental design and organization. GMD 9(5):1937–1958, https://doi.org/10.5194/gmd-9-1937-2016

Eyring V, Flato G, Meehl J, Senior C, Stevens B, Stouffer R, Taylor K (2018) Overview of the Coupled Model Intercomparison Project Phase 6 (CMIP6) Experimental Design and Organization. https://www.wcrp-climate.org/images/modelling/WGCM/CMIP/CMIP6FinalDesign_GMD_180329.pdf, accessed: 2020–11-13

Flynn CM, Mauritsen T (2020) On the climate sensitivity and historical warming evolution in recent coupled model ensembles. Atmos Chem Phys 20(13):7829–7842, https://doi.org/10.5194/acp-20-7829-2020

Førland EJ, Benestad R, Hanssen-Bauer I, Haugen JE, Skaugen TE (2011) Temperature and precipitation development at Svalbard 1900–2100. Adv Meteorol 2011, https://doi.org/10.1155/2011/893790

Freud E, Krejci R, Tunved P, Leaitch R, Nguyen QT, Massling A, Skov H, Barrie L (2017) Pan- Arctic aerosol number size distributions: seasonality and transport patterns. Atmos Chem Phys 17(13):8101–8128, https://doi.org/10.5194/acp-17-8101-2017

Gerland S, Pavlova O, Divine D, Negrel J, Dahlke S, Johansson AM, Maturilli M, Semmling M (2020) Long-term monitoring of landfast sea-ice extent and thickness in Kongsfjorden, and related applications (FastIce). In: Van den Heuvel et al. (eds): SESS report 2019, Svalbard Integrated Arctic Earth Observing System, Longyearbyen, pp 160–167. https://sios-svalbard.org/SESS_Issue2

Gilardoni S, Lupi A, Mazzola M, Cappelletti DM, Moroni B, Ferrero L, Markuszewski P, Rozwadowska A, Krecji R, Zieger P, Tunved P, Karlsson L, Vratolis S, Eleftheriadis K, Viola AP (2020) Atmospheric black carbon in Svalbard. In: Van den Heuvel et al. (eds): SESS report 2019, Svalbard Integrated Arctic Earth Observing System, Longyearbyen, pp 196–211. https://sios-svalbard.org/SESS_Issue2

Graff LS, Iversen T, Bethke I, Debernard JB, Seland Ø, Bentsen M, Kirkevåg A, Li C, Olivié DJL (2019) Arctic amplification under global warming of 1.5 and 2°C in NorESM1-Happi. ESD 10(3):569–598, https://doi.org/10.5194/esd-10-569-2019

Hanssen-Bauer I, Førland E, Hisdal H, Mayer S, AB S, Sorteberg A (2019) Climate in Svalbard 2100. A knowledge base for climate adaptation

Hartmann D, Tank A, Rusticucci M, Alexander L, Brönnimann S, Charabi Y, Dentener F, Dlugokencky E, Easterling D, Kaplan A, et al. (2013) Observations: Atmosphere and surface: Climate Change 2013 the Physical Science Basis: Working Group I Contribution to the Fifth Assessment Report of the Intergovernmental Panel on Climate Change. Cambridge University Press p 159

Held IM, Soden BJ (2006) Robust Responses of the Hydrological Cycle to Global Warming. J Clim 19(21):5686–5699, https://doi.org/10.1175/JCLI3990.1

Hussain M, Mahmud I (2019) pyMannKendall: a python package for non parametric Mann Kendall family of trend tests. J Open Source Softw 4(39):1556, http://dx.doi.org/10.21105/joss.01556

Isaksen K, Nordli Ø, Førland EJ, Łupikasza E, Eastwood S, Niedźwiedź T (2016) Recent warming on Spitsbergen—influence of atmospheric circulation and sea ice cover. J Geophys Res: Atmos 121(20):11,913–11,931, https://doi.org/10.1002/2016JD025606

Karlin S (1983) quote from the 11th R. A. Fisher Memorial Lecture at the Royal Society of London on 20 April 1983

Kendall M (1975) Rank correlation methods (4th edn.) charles griffin. San Francisco, CA 8

Killie MA, Aaboe S, Isaksen K, Van Pelt W, Pedersen ÅØ, Luks B (2021) Svalbard snow and sea-ice cover: comparing satellite data, on-site measurements, and modelling results. In: Moreno-Ibáñez et al (eds) SESS report 2020, Svalbard Integrated Arctic Earth Observing System, Longyearbyen, pp 220-235. https://doi.org/10.5281/zenodo.4293804

Kim KY, Kim JY, Kim J, Yeo S, Na H, Hamlington BD, Leben RR (2019) Vertical feedback mechanism of winter Arctic amplification and sea ice loss. Sci Rep 9(1):1–10, https://doi.org/10.1038/s41598-018-38109-x

Kosaka Y, Xie SP (2013) Recent global-warming hiatus tied to equatorial Pacific surface cooling. Nature 501(7467):403–407, https://doi.org/10.1038/nature12534

Lee S, Gong T, Feldstein SB, Screen JA, Simmonds I (2017) Revisiting the Cause of the 1989–2009 Arctic Surface Warming Using the Surface Energy Budget: Downward Infrared Radiation Dominates the Surface Fluxes. Geophys Res Lett 44(20):10,654–10,661, https://doi.org/10.1002/2017GL075375

Liang YC, Kwon YO, Frankignoul C, Danabasoglu G, Yeager S, Cherchi A, Gao Y, Gastineau G, Ghosh R, Matei D, Mecking JV, Peano D, Suo L, Tian T (2020) Quantification of the Arctic Sea Ice-Driven Atmospheric Circulation Variability in Coordinated Large Ensemble Simulations. Geophys Res Lett 47(1):e2019GL085397, https://doi.org/10.1029/2019GL085397

Mahajan S, Zhang R, Delworth TL (2011) Impact of the Atlantic meridional overturning circulation (AMOC) on Arctic surface air temperature and sea ice variability. J Clim 24(24):6573–6581, https://doi.org/10.1175/2011JCLI4002.1

Mann H (1945) Non-parametric tests against trend. Econmetrica 13:245 – 259

Mann HB, Whitney DR (1947) On a test of whether one of two random variables is stochastically larger than the other. Ann Math Statist 18(1):50–60, https://doi.org/10.1214/aoms/1177730491

Medhaug I, Stolpe MB, Fischer EM, Knutti R (2017) Reconciling controversies about the 'global warming hiatus'. Nature 545(7652):41–47, https://doi.org/10.1038/nature22315

Meier WN, Hovelsrud GK, van Oort BE, Key JR, Kovacs KM, Michel C, Haas C, Granskog MA, Gerland S, Perovich DK, Makshtas A, Reist JD (2014) Arctic sea ice in transformation: A review of recent observed changes and impacts on biology and human activity. Rev Geophys 52(3):185–217, https://doi.org/10.1002/2013RG000431

Navarro JA, Varma V, Riipinen I, Seland Ø, Kirkeva˚ g A, Struthers H, Iversen T, Hansson HC, Ekman AM (2016) Amplification of Arctic warming by past air pollution reductions in Europe. Nat Geoscience 9(4):277–281, https://doi.org/10.1038/ngeo2673

Nordli Ø, Wyszyn´ski P, Gjelten HM, Isaksen K, Łupikasza E, Niedz´wiedz´ T, Przybylak R (2020) Revisiting the extended Svalbard Airport monthly temperature series, and the compiled corresponding daily series 1898–2018. Polar Res 39, https://doi.org/10.33265/polar.v39.3614

Notz D, Marotzke J (2012) Observations reveal external driver for Arctic sea-ice retreat. Geophys Res Lett 39(8):L08502, https://doi.org/10.1029/2012GL051094, l08502

Nummelin A, Li C, Hezel PJ (2017) Connecting ocean heat transport changes from the midlatitudes to the Arctic Ocean. Geophys Res Lett 44(4):1899–1908, https://doi.org/10.1002/2016GL071333

O'Neill BC, Tebaldi C, van Vuuren DP, Eyring V, Friedlingstein P, Hurtt G, Knutti R, Kriegler E, Lamarque JF, Lowe J, Meehl GA, Moss R, Riahi K, Sanderson BM (2016) The Scenario Model Intercomparison Project (ScenarioMIP) for CMIP6. GMD 9(9):3461–3482, https://doi.org/10.5194/gmd-9-3461-2016

Pithan F, Mauritsen T (2014) Arctic amplification dominated by temperature feedbacks in contemporary climate models. Nat Geoscience 7(3):181–184, https://doi.org/10.1038/NGEO2071

Sand M, Berntsen TK, Seland Ø, Kristjánsson JE (2013) Arctic surface temperature change to emissions of black carbon within Arctic or midlatitudes. J Geophys Res: Atmos 118(14):7788–7798, https://doi.org/10.1002/jgrd.50613

Schmeisser L, Backman J, Ogren JA, Andrews E, Asmi E, Starkweather S, Uttal T, Fiebig M, Sharma S, Eleftheriadis K, et al. (2018) Seasonality of aerosol optical properties in the Arctic. Atmos Chem Phys 18(16):11599–11622, https://dx.doi.org/10.5194/acp-18-11599-2018

Screen JA, Blackport R (2019) How Robust is the Atmospheric Response to Projected Arctic Sea Ice Loss Across Climate Models? Geophys Res Lett 46(20):11406–11415, http://doi.org/10.1029/2019GL084936

Screen JA, Simmonds I (2010) The central role of diminishing sea ice in recent Arctic temperature amplification. Nature 464(7293):1334–1337, https://doi.org/10.1038/nature09051

Serreze M, Barrett A, Stroeve J, Kindig D, Holland M (2009) The emergence of surface-based arctic amplification. The Cryosphere 3(1):11

Serreze MC, Barry RG (2011) Processes and impacts of arctic amplification: A research synthesis. Glob Planet Change 77(1):85 – 96, https://doi.org/10.1016/j.gloplacha.2011.03.004

Serreze MC, Barrett AP, Stroeve J (2012) Recent changes in tropospheric water vapor over the Arctic as assessed from radiosondes and atmospheric reanalyses. J Geophys Res: Atmos 117(D10):D10104, https://doi.org/10.1029/2011JD017421

Shaw TA, Baldwin M, Barnes EA, Caballero R, Garfinkel CI, Hwang YT, Li C, O'Gorman PA, Rivière G, Simpson IR, Voigt A (2016) Storm track processes and the opposing influences of climate change. Nat Geoscience 9:656–664, http://dx.doi.org/10.1038/ngeo2783

Shu Q, Wang Q, Song Z, Qiao F, Zhao J, Chu M, Li X (2020) Assessment of Sea-ice extent in CMIP6 With Comparison to Observations and CMIP5. Geophys Res Lett 47(9):e2020GL087965, https://doi.org/10.1029/2020GL087965

Simpkins G (2017) Snapshot: Extreme Arctic heat. Nat Clim Change 7(2):95–95, https://doi.org/10.1038/nclimate3213

Smith DM, Screen JA, Deser C, Cohen J, Fyfe JC, García-Serrano J, Jung T, Kattsov V, Matei D, Msadek R, Peings Y, Sigmond M, Ukita J, Yoon JH, Zhang X (2019) The Polar Amplification Model Intercomparison Project (PAMIP) contribution to CMIP6: investigating the causes and consequences of polar amplification. GMD 12(3):1139–1164, https://doi.org/10.5194/gmd-12-1139-2019

Sipilä M, Hoppe CJM, Viola A, Mazzola M, Krejci R, Zieger P, Beck L, Petäjä T (2020) Multidisciplinary research on biogenically driven new particle formation in Svalbard. In: Van den Heuvel et al. (eds): SESS report 2019, Svalbard Integrated Arctic Earth Observing System, Longyearbyen, pp 168–195. https://sios-svalbard.org/SESS_Issue2

Stroeve J, Notz D (2018) Changing state of Arctic sea ice across all seasons. Environ Res Lett 13(10):103001, https://doi.org/10.1088/1748-9326/aade56

Traversi R, Becagli S, Severi M, Caiazzo L, Mazzola M, Lupi A, Fiebig M, Hermansen O, Krejci R (2021) Arctic haze in a climate changing world: the 2010-2020 trend. In: Moreno-Ibáñez et al (eds) SESS report 2020, Svalbard Integrated Arctic Earth Observing System, Longyearbyen, pp 104-117. https://doi.org/10.5281/zenodo.4293826

Winton M (2011) Do Climate Models Underestimate the Sensitivity of Northern Hemisphere Sea Ice Cover? J Clim 24(15):3924–3934, https://doi.org/10.1175/2011JCLI4146.1

Zhang X, Sorteberg A, Zhang J, Gerdes R, Comiso JC (2008) Recent radical shifts of atmospheric circulations and rapid changes in Arctic climate system. Geophys Res Lett 35(22):L22701, https://doi.org/10.1029/2008GL035607

Zhang X, He J, Zhang J, Polyakov I, Gerdes R, Inoue J, Wu P (2013) Enhanced poleward moisture transport and amplified northern high-latitude wetting trend. Nat Clim Change 3(1):47–51, https:// doi.org/10.1038/nclimate1631